The EMBO Journal vol.4 no.7 pp.1793-1798, 1985

Proviral activation of the putative oncogene *Pim*-1 in MuLV induced T-cell lymphomas

Gerard Selten, H. Theo Cuypers and Anton Berns

Department of Biochemistry, University of Nijmegen, Geert Grooteplein N21, 6525 EZ, Nijmegen, The Netherlands

Communicated by H.Bloemendal

Proviral integration near the *Pim*-1 gene is frequently observed in murine leukemia virus induced T-cell lymphomas in mice. Integration in the *Pim*-1 domain is associated with the presence of enhanced levels of a *Pim*-1 mRNA, which is normally expressed as a predominant 2.8 kb species at low levels in lymphoid tissues. The majority of integrations occurred in the 3′ region of the *Pim*-1 transcription unit. This resulted in transcripts ranging in size from 2.0 to 2.6 kb, which were terminated in the 5′ proviral LTR. Dependent on the site of integration up to 1300 bases of *Pim*-1 specific sequences were missing from the modified *Pim*-1 mRNA in these lymphomas.

Key words: insertional mutagenesis/murine leukemia virus/Pim-1/T-cell lymphomas

Introduction

Murine leukemia viruses (MuLVs) are replication-competent retroviruses which lack transforming genes but cause lymphomas after a long latent period (Rowe and Pincus, 1972; Pederson *et al.*, 1980; Nobis and Jaenisch, 1980; Steffen and Weinberg, 1978). Tumor induction by the slow transforming retroviruses most likely depends on activation of cellular genes by integrated proviruses. Activation of the c-*myc* proto-oncogene by proviral DNA insertion has been described in avian leukosis virus (ALV) induced B-cell lymphomas in birds (Hayward *et al.*, 1981; Neel *et al.*, 1981; Payne *et al.*, 1982; Westaway *et al.*, 1984), in MuLV induced T-cell lymphomas in mice (Corcoran *et al.*, 1984; Selten *et al.*, 1984), and in feline leukemia virus (FeLV) induced lymphomas in cats (Neil *et al.*, 1984). A similar mechanism underlies the activation of c-*erb* in ALV induced erythroblastosis (Fung *et al.*, 1983), and the activation of the *int*-1 and *int*-2 genes in mouse mammary tumor virus (MMTV) induced mammacarcinomas in mice (Nusse and Varmus, 1982; Nusse *et al.*, 1984; Peters *et al.*, 1983; Dickson *et al.*, 1984).

Integrated proviruses can activate flanking cellular genes either by transcription from the viral promoter (Hayward *et al.*, 1981; Neel *et al.*, 1981; Payne *et al.*, 1982; Westaway *et al.*, 1984; Cullen *et al.*, 1984), by virtue of the enhancer activity of proviral sequences on adjacent cellular promoters (Corcoran *et al.*, 1984; Nusse *et al.*, 1984; Dickson *et al.*, 1984; Cuypers *et al.*, 1984; Selten *et al.*, 1984), or by disruption of *cis*-controlling elements (Leder *et al.*, 1983). Furthermore, integration of proviruses within the transcription unit may modify the structure, and thereby the biological characteristics, of the encoded protein. The activation of c-*myc* by ALV proviruses occurs predominantly by deleted proviruses inserted upstream from the *myc* gene in the same transcriptional orientation (Neel *et al.*, 1981; Payne *et al.*, 1982). In contrast, the activation of c-*myc* in MuLV induced T-cell lymphomas is mediated predominantly by proviruses integrated upstream of c-*myc* in the opposite transcriptional orientation (Corcoran *et al.*, 1984; Selten *et al.*, 1984), whereas the activation of *int*-1 and *int*-2 in MMTV induced mammacarcinomas involves proviruses integrated either upstream or downstream of the *int*-1 and *int*-2 genes with a transcriptional orientation which is directed away from the *int* genes (Nusse *et al.*, 1984; Dickson *et al.*, 1984). Recently we have described the frequent integration of proviruses in the *Pim*-1 domain in MuLV induced T-cell lymphomas (Cuypers *et al.*, 1984). Here we describe the orientation and site of integration of proviruses in additional lymphomas, the tissue specific expression pattern of the *Pim*-1 gene, the mode of activation of *Pim*-1 and the effect of the site of proviral integration on the size and nature of *Pim*-1 mRNA transcripts.

Results

Localization of the Pim-1 transcription unit

The *Pim*-1 gene is expressed at low levels in normal thymus and spleen, and at elevated levels in lymphomas with proviral integration near *Pim*-1 (see below). To locate the *Pim*-1 transcription unit and to determine the direction of transcription, polyA$^+$ RNA derived from normal and lymphoma tissues was hybridized with several probes from the *Pim*-1 region. Hybridization was found with probes A, B, D and E, but not with probe C (see Figure 1g for location of probes). The use of single strand M13 probes from the *Pim*-1 region revealed that the direction of transcription was from left to right on the *Pim*-1 map. Furthermore, S1 nuclease analyses, using subclones from the *Pim*-1 region, indicated that at least 80% of the *Pim*-1 mRNA sequence is encoded in the region between position −6 and +1 on the *Pim*-1 map. The location and transcriptional direction of the *Pim*-1 transcription unit is visualized by the large horizontal arrow in Figure 1g. The dotted lines indicate that the initiation- and termination-site(s) of the *Pim*-1 transcription unit are still unsettled.

Position and orientation of proviruses in the Pim-1 region

Proviral integration near *Pim*-1 or c-*myc* is observed with high frequency in MuLV induced T-cell lymphomas which develop after a latency of less than six months (Cuypers *et al.*, 1984). We have extended our earlier study by analyzing additional fast developing lymphomas induced in BALB/c mice by infection of newborns with Moloney MuLV. A total of 31 out of 66 mice which developed lymphomas within six months, contained a provirus integrated in the *Pim*-1 region, whereas only five out of 64 mice which developed disease after more than six months, had a proviral insertion near *Pim*-1. The sites of proviral integration as well as the transcriptional orientation of the proviruses with respect to the *Pim*-1 gene were determined by Southern blot analysis of lymphoma DNAs digested with *Eco*RI, *Eco*RV and *Pvu*II, using probes specific for *Pim*-1 and the Moloney U3LTR. In Figure 1 the proviral integration sites and the transcription orientations of proviruses with respect to the *Pim*-1 gene are shown in detail for a number of lymphomas. Southern blot analysis of *Eco*RV digested lymphoma DNA with specific *Pim*-1

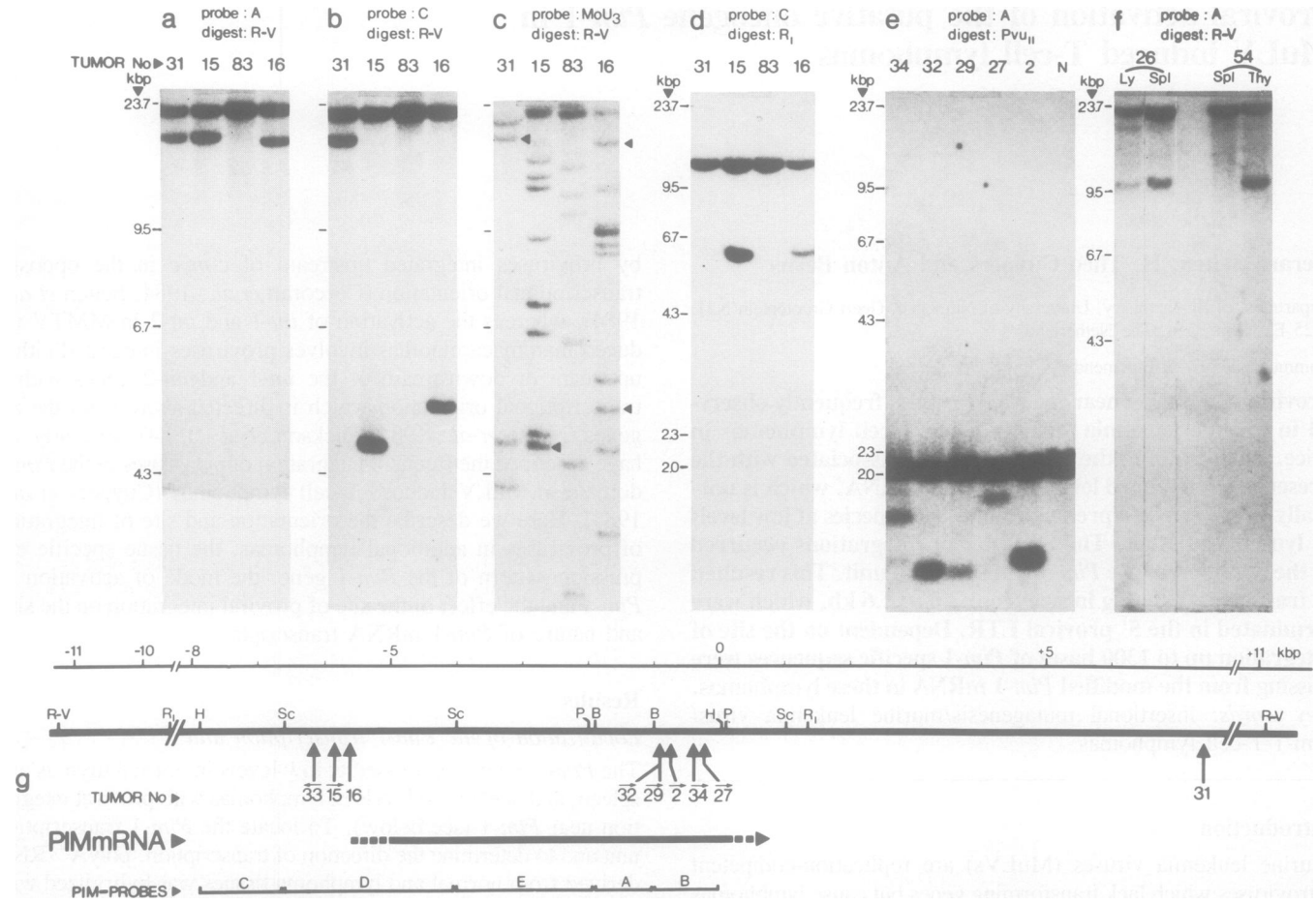

Fig. 1. Southern blot analysis of lymphoma DNA with specific *Pim*-1 and proviral probes. 10 μg of lymphoma DNA, obtained from spleen (spl), thymus (thy), peripheral lymphnodes (Ly) or normal mouse (BALB/c) tissue (N) were digested with restriction endonucleases *Eco*RV (**a,b,c,f**), *Eco*RI (**d**) or *Pvu*II (**e**), separated on 0.6% agarose gels, transferred to nitrocellulose filters and annealed to probe A (**a,e,f**), probe C (**b,d**), or to the Moloney U3LTR (MoU3LTR) probe. Autoradiographs **a,b** and **c** were obtained from the same filter with the probes indicated above the panels. The location of *Pim*-1 specific probes A-E is shown in **g**. A physical map of the *Pim*-1 region, as well as the position and orientation of the proviruses in the *Pim*-1 region of lymphomas analyzed in panels **a**–**e**, are presented in **g**. The integration site of the provirus in tumor 1 is defined as position 0. Small horizontal arrows above tumor numbers indicate the direction of transcription of the integrated provirus (5′--> 3′). Localization of *Pim*-1 transcription unit and direction of transcription is indicated by the large horizontal arrow. Dotted line reflects the fact that the beginning and end of the *Pim*-1 transcription unit is still uncertain. Abbreviations used: RV, *Eco*RV; RI, *Eco*RI; H, *Hind*III; Sc, *Sac*I; P, *Pvu*II; B, *Bam*HI.

probes (Figure 1g) results in the recognition of a 22 kb fragment, corresponding with the unaltered allele, and the detection of an additonal fragment (e.g. lymphomas 31, 15 and 16, Figure 1a and 1b), corresponding with the allele in which the provirus is inserted between position −11 and +11 on the physical map of *Pim*-1. The size of the additional fragments detected after blot hybridization using various restriction endonucleases and different *Pim*-1 probes establish the proviral localization within the *Pim*-1 domain. Since proviruses harbor *Eco*RV recognition sites in their LTRs, Southern blot analyses of *Eco*RV digested DNA from lymphoma 15, 16 and 31 with *Pim*-1 probes A and C (Figure 1a and 1b) map the provirus in these lymphomas at position −5.9, −5.7 and +7.5, respectively. Hybridization of *Eco*RI digested DNAs from the same lymphomas with probe C confirms the proviral integration sites in lymphomas 15 and 16 (Figure 1d). Besides the 11 kbp *Eco*RI fragment from the unaltered allele, an additional *Eco*RI fragment was observed in DNA from lymphoma 15 and 16. In lymphoma 31 no additional *Eco*RI fragment was detected by probe C, as the provirus in this tumor was inserted outside the region corresponding with the 11 kb *Eco*RI fragment.

Evidence that the observed alterations in the *Pim*-1 region are indeed the result of proviral integrations was obtained by hybridizing the same Southern blots with a specific Moloney U3LTR probe. Additional fragments detected by hybridization with probe A and C (Figure 1a and 1b) also annealed with the MoU3LTR probe (see arrows in Figure 1c). A more detailed mapping of proviruses integrated in the 3′ region of the *Pim*-1 gene is shown in Figure 1e. Southern blot analysis of *Pvu*II digested lymphoma DNAs with probe A results both in the recognition of a 2.1 kbp fragment corresponding with the unaltered allele, as well as the detection of novel DNA fragments of 1.7, 1.0, 1.0, 1.8 and 1.1 kbp in lymphoma 34, 32, 29, 27 and 2, respectively. Since these proviruses contain a *Pvu*II site in their LTR (Van Beveren *et al.*, 1982), the fragment sizes observed after *Pvu*II digestion map these proviruses as depicted in Figure 1g.

In DNA of 32 lymphomas, proviruses were found in the 3′ domain of the *Pim*-1 gene (Figure 2), and in three lymphomas the proviruses were localized in the 5′ region of the *Pim*-1 gene. A total of 24 out of the 32 proviruses, which were integrated near the 3′ end of the *Pim*-1 gene, were localized between map position −1 and +1 and possessed the same transcriptional orien-

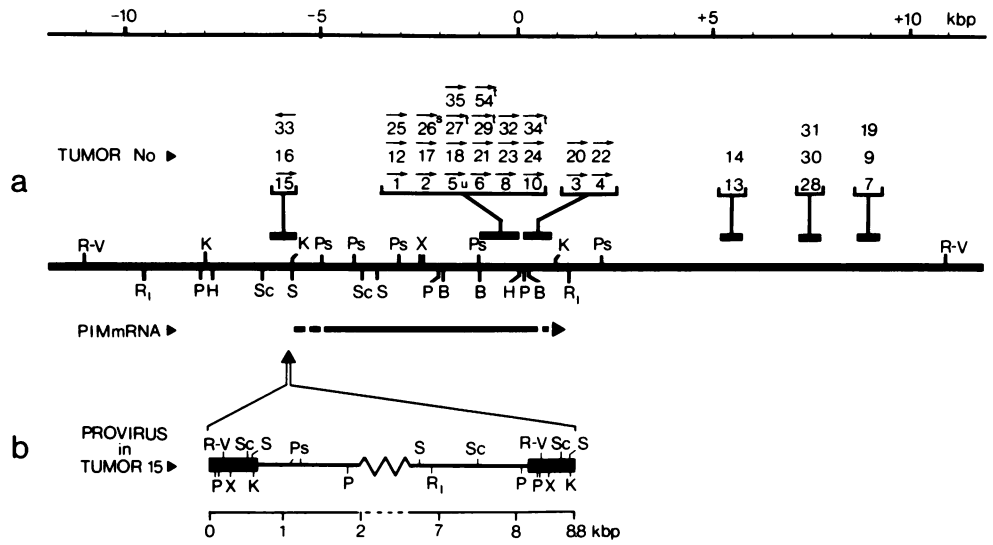

Fig. 2. Location and orientation of proviral integrations in the *Pim*-1 region. (**a**) Horizontal arrows above tumor numbers denote the orientation of the integrated provirus (5'--> 3'), boxes show the position of integrated proviruses within the *Pim*-1 region. In those instances in which the orientation of the provirus could not be confirmed by blot hybridization after cleavage with a different enzyme, no orientation is indicated. Localization of *Pim*-1 mRNA sequences and direction of transcription are indicated by the large horizontal arrow (5'--> 3'). In case the proviral integration pattern differed among lymphoma tissues within the same animal, the tissue is indicated: t: thymus; s: spleen. (**b**) A detailed restriction endonuclease map of the integrated provirus of tumor 15 at position −5.9 on the *Pim*-1 map. Abbreviations: see legend to Figure 1, and S, *Sma*I; K, *Kpn*I; Ps, *Pst*I; X, *Xba*I.

tation as *Pim*-1 ; in eight lymphomas the provirus was inserted downstream from the *Pim*-1 gene between map position +5 and +9. Three lymphomas (15, 16 and 33) contained proviruses close to map position −6 in the 5' region of the *Pim*-1 gene. In nearly all instances the orientation of the provirus could be established unambiguously. However, in lymphoma 16, the U3LTR probe recognized identical sized fragments as *Pim*-1 probes A and C (Figure 1c). Also analysis with other enzymes did not allow the determination of the proviral orientation in tumor 16. Since the proviruses, which were integrated downstream from map position 1.3 (*Eco*RI), could only be detected after digestion with *Eco*RV, the orientation is not given, although hybridization analyses using a U3LTR probe indicated that probably all these proviruses have the same transcriptional orientation as *Pim*-1 (data not shown). Figure 2a presents an overview of the integration sites and transcriptional orientation of the proviruses in the *Pim*-1 region. In some lymphomas the anatomical location of the tumor is indicated, as in these instances the integration pattern differed between tissues as the result of the oligoclonal origin of these tumors (e.g., Figure 1f, lymphoma 26 and 54; see also Selten *et al.*, 1984).

To search for possible proviral integrations further upstream (beyond position −10), specific cellular probes were prepared from genomic DNA clones, comprising the region between −30 and −10 kbp on the map of *Pim*-1 . No additional integrations or alterations were found in the −10 to −30 kbp region in any of the 130 lymphomas analyzed. No *Pim*-1 probes are available so far to detect proviral integrations downstream from position +11.

Structure of integrated proviruses

Both mink cell focus-inducing (MCF) proviruses as well as ecotropic proviruses were found integrated in the *Pim*-1 domain. Approximately 80% of the proviruses exhibited an MCF structure, as revealed by the presence of an *Eco*RI site at position 6.9 on the proviral genomic map (Quint *et al.*, 1981; van der Putten *et al.*, 1981). In lymphomas 3, 8, 12, 23, 32 and 33 the *Eco*RI site was absent, suggesting integration of ecotropic proviruses near *Pim*-1 in these lymphomas.

Proviruses in lymphomas 15 and 16, which are integrated in the 5' region of the *Pim*-1 gene, showed internal deletions of 4.5 and 3 kbp, respectively. The provirus in lymphoma 15 showed the same transcriptional orientation as the *Pim*-1 transcript, and therefore might represent an example of promoter insertion. This provirus with adjacent *Pim*-1 sequences was molecularly cloned in phage lambda. In Figure 2b the physical map of the cloned provirus is shown. The proviral integration in lymphoma 15 was mapped at position −5.9. The restriction sites *Pvu*II, *Xba*I, *Sst*I, *Sma*I, *Eco*RV and *Kpn*I were found to be present in both LTRs (van Beveren *et al.*, 1980). The LTR-specific fragments generated by these enzymes indicated that as in one of the proviruses cloned from the 3' region (Berns *et al.*, 1983; van Beveren *et al.*, 1982), this provirus contained two intact LTRs with duplicated enhancer sequences in the U3 region. *Xba*I and *Kpn*I digestion gave rise to a single internal proviral fragment of 3.7 kbp, indicating the presence of a deletion of 4.5 kbp in this provirus. The absence of recognition sites for restriction endonucleases *Xho*I, *Bam*HI, *Bgl*II and *Hind*III located this deletion between map position 1.8 (*Pvu*II) and 6.8 (*Sma*I) on the physical map of Moloney MCF (Bosselman *et al.*, 1982). Further analysis of lymphoma 16 showed that the provirus in this tumor contained a deletion ~3 kbp (data not shown).

Proviral insertion enchances Pim-1 transcription

To investigate whether proviral insertion near or in the *Pim*-1 gene affects the level of *Pim*-1 mRNA, polyA$^+$ RNA was isolated from lymphoma tissues and the amount of *Pim*-1 mRNA estimated by the dot-blot hybridization technique. Examples of *Pim*-1 mRNA levels in normal and tumor tissues are shown in Figure 3. As a control for the integrity and amount of spotted polyA$^+$ RNA, hybridization with an actin probe is included. In polyA$^+$ RNA samples of lymphomas bearing a provirus near *Pim*-1 (lymphomas 2, 15, 16, 26, 27t, 28, 29, 30, 31, 32 and 54t, marked with an asterix) the *Pim*-1 mRNA levels were

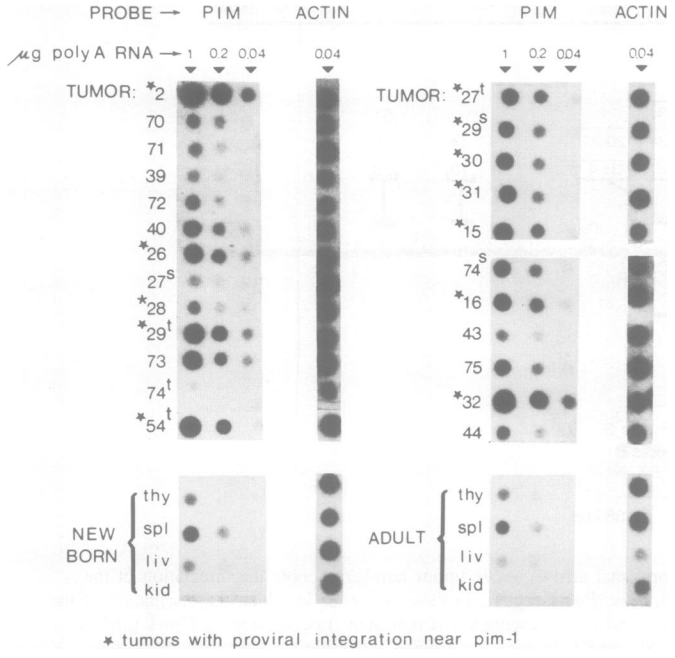

Fig. 3. Expression of *Pim*-1 sequences in lymphoma and normal tissues. Several dilutions ranging from 1 to 0.04 μg polyA$^+$ RNA from 24 randomly chosen lymphomas (t: thymus; s: spleen) and from newborn and adult tissues were applied to nitrocellulose filters and hybridized to ^{32}P-labeled probe A. An actin probe was used as a control for the quantity and integrity of the RNA samples. Tumor numbers marked by an asterix denote lymphomas with a proviral integration in the *Pim*-1 region (see Figure 2). The lower panels of the figure show expression levels of *Pim*-1 in polyA$^+$ RNA from normal thymus (thy), spleen (spl), liver (liv) and kidney (kid) of newborn (1−4 days) and adult (3 months) BALB/c mice.

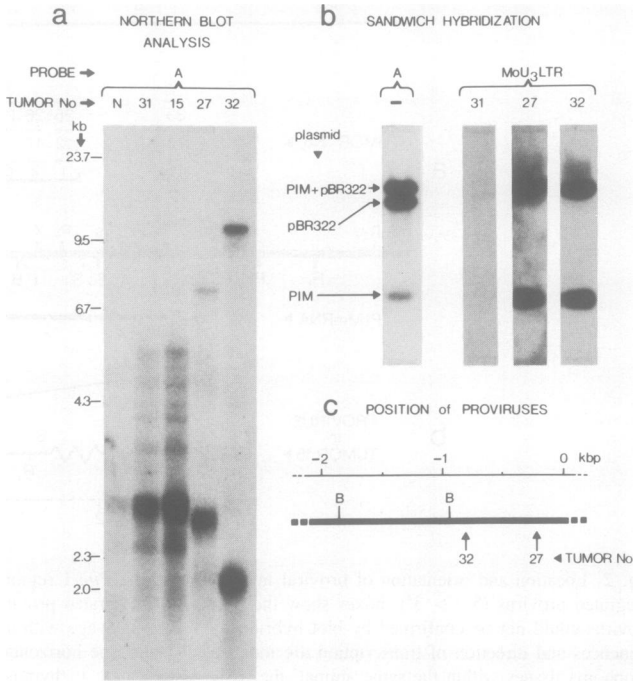

Fig. 4. Analysis of *Pim*-1 transcripts. (**a**) Northern blot analysis of polyA$^+$ RNA from newborn spleen (N, 3 μg), and lymphomas 31 (5 μg), 15 (5 μg), 27 (2 μg) and 32 (2 μg). Glyoxal treated RNAs and marker DNAs (*Hind*III digested λ DNA) were separated on 1% agarose gels, transferred to nitrocellulose filters and hybridized to ^{32}P-labeled probe A. (**b**) Demonstration of covalent linkage of U3LTR sequences to *Pim*-1 transcripts. Filters containing *Eco*RI and *Bam*HI digested probe A plasmid were hybridized to ^{32}P-labeled plasmid probe A ("-", left panel). Filters incubated with polyA$^+$ RNA from lymphomas 27, 31 or 32 were subsequently annealed to ^{32}P-labeled MoU3LTR probe (right panel). (**c**) Drawing showing position of proviruses in lymphomas 27 and 32 in the 3′ region of the *Pim*-1 gene (position −0.2 and −0.8 on the *Pim*-1 map, respectively). Details concerning lymphomas 15 and 31 are shown in Figure 1. Abbreviations: see legend to Figure 1.

significantly elevated as compared with the levels of *Pim*-1 mRNA in lymphomas without proviral integration near the *Pim*-1 gene. In a few tumors increased levels of *Pim*-1 mRNA was observed without the concomittant integration of a provirus (e.g., lymphoma 73). In these lymphomas either proviral integration occurred outside the examined 40 kbp region (−30 to +11 kbp on the *Pim*-1 map), or other mechanisms for the activation of *Pim*-1 are involved.

The amount of *Pim*-1 mRNA appeared dependent on the site of proviral integration. In tumors with a provirus in the −1 to 0 region, *Pim*-1 mRNA levels were significantly higher (e.g., lymphomas 2, 26, 27t, 29, 32 and 54t) than in tumors in which the provirus was integrated in the 5′ region (lymphomas 15 and 16) or far downstream of the *Pim*-1 gene (e.g., lymphomas 28, 30 and 31). This effect was even more pronounced when the expression level was adjusted by taking into consideration the intensity of the additional hybridizing bands on Southern blots, or by comparing the expression levels of monoclonal tumors obtained after transplantation of primary lymphomas (data not shown).

The level of expression varies in tumor tissues obtained from different anatomical sites (compare tumors 27, 29 and 74, Figure 3). A higher level of expression in these tumors is associated with a more pronounced hybridizing modified *Pim*-1 allele. In lymphoma 27 enhanced *Pim*-1 expression was seen in the thymus but not in the spleen. In accordance with this observation proviral integration was only detectable in the thymic lymphoma. In almost all lymphomas without proviral integration near *Pim*-1, the *Pim*-1 mRNA contents were comparable with the levels in normal lymphatic tissues. Exceptions are lymphomas 27s and 74t, in which expression was hardly detectable.

In RNA isolated from newborn and adult mice, *Pim*-1 mRNA transcripts are predominantly found in spleen and thymus. Minor amounts are detectable in liver and no *Pim*-1 transcripts are present in kidney RNA (Figure 3, lower panels). No *Pim*-1 mRNA transcripts were detected in RNA from newborn and adult brain, lung, heart, ovaries and testes. During embryonic development *Pim*-1 expression is mostly restricted to liver, thymus and spleen (data not shown). In liver the highest levels are seen around day 16−19 of gestation, for the thymus around birth, whereas *Pim*-1 mRNA levels in spleen increase steadily up to 14 days after birth. Also in the 10−12 days old placenta a high expression level is observed.

Nature of Pim-1 transcripts

Northern blot analysis of polyA$^+$ RNA, isolated from normal tissues or lymphomas with a proviral integration around position −6 (e.g., lymphoma 15) or downstream of position +1 (e.g., lymphoma 31) on the *Pim*-1 map, showed a 2.8 kb (the predominant species) and a 2.45 kb *Pim*-1 mRNA (see Figure 4a). Because total cellular RNA was isolated, *Pim*-1 precursors were also detected.

Proviral integrations in the 0 to −1 region of the *Pim*-1 domain affected the size of the *Pim*-1 mRNA. Northern blot analyses of polyA$^+$ RNA of these lymphomas showed smaller transcripts ranging in size from 2.0 to 2.6 kb (e.g., lymphomas 27 and 32 in Figure 4a). Also larger (up to 10 kb) transcripts were found

in some of these tumors (lymphoma 32, Figure 4a). They most likely represent read-through products in which proviral RNA is covalently linked to the 3′ end of the *Pim*-1 mRNA.

Integration of a provirus in the 3′ region of the *Pim*-1 gene not only results in a reduction in size of the *Pim*-1 mRNA but also in the linking of LTR sequences to the *Pim*-1 transcript. Sandwich hybridization with RNA from lymphomas 27 and 32 showed that *Pim*-1 transcripts were terminated in the 5′LTR of the integrated provirus. Nitrocellulose filters containing a mixture of *Bam*HI and *Eco*RI cleaved probe A plasmid, giving rise to fragments of 5.2 kbp (pBR322 + *Pim*-1), 4.3 kbp (pBR322) and 0.9 kbp (*Pim*-1), were successively hybridized with lymphoma polyA$^+$ RNA and a ^{32}P-labeled Moloney U3LTR probe (Figure 4b). The results indicate that in lymphomas 27 and 32, but not in lymphoma 31, viral sequences are covalently linked to *Pim*-1 mRNA transcripts. Disruption of *Pim*-1 mRNA sequences by termination in the integrated proviral LTR is observed in over 60% of the lymphomas with proviral integration in the *Pim*-1 region.

Integrations around position −6 did not affect the size of the *Pim*-1 mRNA. In tumor 33 a provirus was integrated at position −6.2 with a transcriptional orientation opposite to *Pim*-1. Activation of *Pim*-1 transcription in this tumor is likely to be mediated by enhancement. Therefore, the normal functional *Pim*-1 promoter is expected to be located to the right of position −6. Also the mature *Pim*-1 mRNAs in tumor 15, in which the provirus was integrated in the 'promoter insertion' orientation, were of similar size as the mRNAs in normal spleen and lymphoma 31 (Figure 4a). To verify whether transcription was initiated from a proviral LTR, sandwich hybridization was performed, as described for lymphomas with inserted proviruses in the 3′ region of the *Pim*-1 gene (Figure 4b). For this analysis a Moloney U5LTR probe was used. However, no U5LTR sequences were found to be linked to *Pim*-1 transcripts in tumor 15 (data not shown). This observation, and the fact that lymphomas 33, 15 and 16 have identical sized *Pim*-1 transcripts (despite their opposite proviral orientation), suggests that the *Pim*-1 promoter is probably located downstream from position −6. This was further supported by the observation that promoter-like sequences were found in this region (data not shown). However, we have not formally excluded the possibility that the integration region around position −6 is part of a *Pim*-1 intron.

Discussion

Position of proviruses in the Pim-1 domain

The activation of c-*myc* by ALV in bursal lymphomas is mediated predominantly by insertion of a viral promoter upstream of the c-*myc* coding sequence (Hayward *et al.*, 1981, 1981; Neel *et al.*, 1981; Payne *et al.*, 1982; Westaway *et al.*, 1984; Cullen *et al.*, 1984). In contrast, in mice the proviral activation of c-*myc* (Corcoran *et al.*, 1984; Selten *et al.*, 1984) as well as the activation of *int*1 (Nusse *et al.*, 1984), *int*-2 (Dickson *et al.*, 1984), and *Pim*-1 occurs almost exclusively by enhancement. The transcriptional orientation of the majority of the proviruses in these mouse tumors is directed away from the activated gene. Even the few proviral integrations in the 5′ region of c-*myc* and *Pim*-1, which have the 'promoter insertion' orientation, seem to activate c-*myc* and *Pim*-1 predominantly by enhancement (Selten *et al.*, 1984).

The position of the integrated proviruses with respect to the cellular promoters differs in the various systems (Corcoran *et al.*, 1984; Selten *et al.*, 1984; Nusse *et al.*, 1984; Dickson *et al.*, 1984; Shih *et al.*, 1984). Whereas in mouse T-cell lymphomas proviral integration near c-*myc* is almost exclusively found in the promoter region of the gene, near *Pim*-1 most integrations occur within the 3′ region of the transcription unit. Several factors may contribute to this integration pattern. Firstly, the preference of the proviral integration machinery for distinct sequences of chromatin structures (Breindl *et al.*, 1984). Secondly, the alterations needed to potentiate a particular proto-oncogene. The second aspect might require the displacement of *cis*-controlling elements as suggested for the activation of c-*myc* upon translocation (Leder *et al.*, 1983), the removal of control elements which might interefere with efficient translation (Miller *et al.*, 1984), or alteration of the gene product as observed for the *ras* proto-oncogene (Tabin *et al.*, 1982; Reddy *et al.*, 1982). These factors could explain the observed clustering of integrations in the *Pim*-1 domain.

Level and nature of Pim-1 mRNA in lymphomas

Proviral integration near *Pim*-1 is always associated with increased *Pim*-1 mRNA levels. In most lymphomas without a proviral insertion near *Pim*-1, mRNA levels were comparable with the levels in normal lymphatic tissues. In a few instances (tumors 73 and 40) enhanced expression was seen without proviral integration near *Pim*-1. In contrast, in the splenic lymphoma of mouse 27, and the thymic lymphoma of mouse 74, *Pim*-1 mRNA was hardly detectable. The primary target cell giving rise to these lymphomas might have belonged to a cell lineage which normally produces only minute amounts of *Pim*-1 mRNA or the level of *Pim*-1 mRNA expression was reduced during the progressive growth of these lymphomas. Similar observations were made for c-*myc* mRNA expression in MuLV induced lymphomas (Selten *et al.*, 1984).

In ~60% of the lymphomas with an activated *Pim*-1 gene, the provirus is integrated in the 3′ region of the *Pim*-1 transcription unit. This results in higher *Pim*-1 mRNA levels than seen in tumors with integrations in other regions of the *Pim*-1 domain. These mRNAs are missing up to 1300 nucleotides of *Pim*-1 specific sequences and contain ~500 nucleotides of LTR sequences at their 3′ ends. Integration in this region could have several effects: (i) it could alter the *Pim*-1 encoded protein, possibly increasing its oncogenic potential. Since proviruses are found integrated throughout this region, and outside the *Pim*-1 gene, truncation of the *Pim*-1 protein by proviral insertion is certainly not essential for the potentiation of *Pim*-1. The absence of integrations in the −1 to −5.5 region suggests that the integrity of that part of the *Pim*-1 gene is required to encode a biological active protein. (ii) It might enhance more effectively transcription from the *Pim*-1 promoter, or increase *Pim*-1 mRNA stability. The significant higher level of *Pim*-1 mRNA transcripts present in lymphomas with an integration in this region of *Pim*-1 as compared with lymphomas with an integration outside the *Pim*-1 gene supports this explanation. (iii) The removal of 3′ sequences could affect the efficiency of translation. Such an effect has recently been described for the *fos* mRNA (Miller *et al.*, 1984). Protein expression studies have to be performed to resolve this issue.

Remarkably, in lymphomas with an altered *Pim*-1 allele (e.g., Figure 4a, tumors 27 and 32) transcription from the normal allele was not observed. Either allelic exclusion prevents transcription from the normal allele as has been suggested for c-*myc* expression (Leder *et al.*, 1983), or expression of the normal allele is inhibited by other mechanisms (compare low levels of *Pim*-1 mRNA in lymphomas 74t and 27s in Figure 3).

The increased level of *Pim*-1 mRNA in tumors with proviral integrations near *Pim*-1 corroborates the notion that a high expression level of a proto-oncogene can confer a selective growth advantage to a cell. The proviral activation of *Pim*-1 in a high percentage of MuLV induced early T-cell lymphomas, and its expression pattern during development, reminiscent for cell lineages of the haemopoietic system, suggest that *Pim*-1 might belong to a specific class of proto-oncogenes with a regulatory role in lympoid cells.

Materials and methods

Mice, viruses and lymphomas

Lymphomas were generated by injecting newborn BALB/c mice with Moloney MuLV clone 1A as described (Jaenisch *et al.*, 1975; Cuypers *et al.*, 1984). Spontaneously developing lymphomas from BALB/Mo and AKR/Fu mice were obtained as described previously (van der Putten *et al.*, 1979; Quint *et al.*, 1981; Cuypers *et al.*, 1984).

Molecular cloning

A 12 kb *Hind*III DNA fragment localized between position −8 and 0 on the *Pim*-1 map, comprising the integrated (deleted) provirus with adjacent cellular *Pim*-1 sequences of lymphoma 15 was molecularly cloned in bacteriophage lambda.

To obtain *Pim*-1 specific probes, comprising the region between map position −10 and −30, 300 μg of high mol. wt. liver DNA (BALB/c) was partially digested with restriction endonuclease *Sau*3A. DNA fragments were separated on size and the 12−20 kbp fragments were cloned in Charon phage 28. Recombinant phage plaques were selected which hybridized to probe C. From a positive reacting clone a single copy probe was obtained, which was located between position −17 and −18 on the *Pim*-1 map.

DNA isolation and restriction enzyme analysis

High mol. wt. DNA from lymphoma tissues was prepared as described (van der Putten *et al.*, 1979). DNA samples of 10 μg were digested as recommended by the suppliers (Amersham, BRL, Boehringer), separated on 0.6% agarose gels, transferred to nitrocellulose filters and hybridized to ^{32}P-labeled probes as described previously (Quint *et al.*, 1981). After hybridization, filters were washed in 0.1 x SSC, 0.1% SDS at 65°C. After hybridization with the Moloney U3LTR probe the final wash was performed at 60°C. To remove hybridized probe, filters were rinsed with 0.2 M alkali. As mol. wt. markers *Hind*III digested phage λ DNA was used.

Preparation of RNA

Frozen tissues were homogenized at 0°C in 3 M LiCl, 6 M urea and maintained overnight at 4°C as described (Auffray and Rougeon, 1980; Selten *et al.*, 1984). Total cellular RNA was obtained after centrifugation at 16 000 *g*. RNA was deproteinized by two successive phenol:chloroform:isoamylalcohol (50:48:2) extractions and precipitated with ethanol. RNA samples were heated at 65°C for five minutes before polyA$^+$ selection on oligo(dT) chromatography.

Northern and dot-blot analysis

For dot-blot analysis, polyA$^+$ RNA was dissolved in distilled water and applied to nitrocellulose filters as described by Muller *et al.* (1982). Glyoxal treatment and Northern blot analysis were carried out as described (Carmichael and McMaster, 1980; Thomas, 1980). Filters were hybridized with ^{32}P-labeled probes as described above for DNA containing filters, including the washing procedures (last washing 0.1 x SSC, 0.1% SDS at 65°C) and exposed to X-ray film. As mol. wt. markers *Hind*III digested λ DNA was used. Denaturation was performed as described for RNA.

Sandwich hybridization

2 μg of plasmid DNA containing probe A insert was cleaved with *Eco*RI and *Bam*HI, respectively. The fragments were mixed, separated on a 0.6% agarose gel and transferred to nitrocellulose. Three fragments were thus obtained: a 5.2 kbp fragment, representing the linearized plasmid, a 4.3 kbp pBR322 fragment, and a 0.9 kbp fragment representing the *Pim*-1 specific insert. Filters were incubated overnight with 5 μg polyA$^+$ RNA under conditions as described (Nusse *et al.*, 1984), washed twice in 0.1 x SSC, 0.1% SDS at 53°C, blotted dry and subsequently annealed to ^{32}P-labeled MoLTR specific probes for 16 h. Filters were washed twice with 0.1 x SSC, 0.1% SDS for 1 h at 53°C, dried and autoradiographed overnight.

Hybridization probes

Isolation of *Pim*-1 specific probes A-E, as well as the MoU3LTR probe was performed as described (Cuypers *et al.*, 1984). The MoU5LTR probe comprises a *Hpa*II fragment from the MSV-12 LTR (van Beveren *et al.*, 1982), subcloned in M13. The actin cDNA clone is described by Dodemont *et al.* (1982).

Acknowledgements

This work was performed in the laboratory of Dr. H. Bloemendal, to whom we are particularly indebted. We appreciated the assistance of the coworkers of the Central Animal Laboratory. We wish to thank Drs. Zijlstra and Melief of the Central Laboratory of the Netherlands Red Cross Blood Transfusion Service for their contributions. This work was supported by grants from the Koningin Wilhelmina Fonds (G.S.) and by the Netherlands Organization for the Advancement of Pure Research (ZWO) through the Foundation for Funadmental Medical Research (FUNGO).

References

Auffrey,C. and Rougeon,F. (1980) *Eur. J. Biochem.*, **107**, 303-314.
Berns,A., Robanus-Maandag,E., van der Putten,H. and Quint,W. (1983) in *Genetic Rearrangements*, Croom Helm, London and Canberra, pp. 93-105.
Bosselman,R.A., van Straaten,F., van Beveren,C., Verma,I.M. and Vogt,M. (1982) *J. Virol.*, **44**, 19-31.
Breindl,M., Harbers,K. and Jaenisch,R. (1984) *Cell*, **38**, 9-16.
Carmichael,G.G. and McMaster,G.K. (1980) *Methods Enzymol.*, **65**, 380-391.
Corcoran,L.M., Adams,J.M., Dunn,A.R. and Cory,S. (1984) *Cell*, **37**, 113-122.
Cullen,B.R., Lomedico,P.T. and Ju,G. (1984) *Nature*, **307**, 241-245.
Cuypers,H.T., Selten,G., Quint,W., Zijlstra,M., Robanus-Maandag,E., Boelens,W., van Wezenbeek,P., Melief,C. and Berns,A. (1984) *Cell*, **37**, 141-150.
Dickson,C., Smith,R., Brookes,S. and Peters,G. (1984) *Cell*, **37**, 529-536.
Dodemont,H.J., Soriano,P., Quax,W.J., Ramaekers,F., Lenstra,J.A., Groenen,M.A., Bernardi,G. and Bloemendal,H. (1982) *EMBO J.*, **1**, 167-171.
Fung,Y.T., Lewis,W.G., Crittenden,L.B. and Kung,H. (1983) *Cell*, **33**, 357-368.
Hayward,W.S., Neel,B.G. and Astrin,S. (1981) *Nature*, **290**, 475-480.
Jaenisch,R., Fan,H. and Croker,B. (1975) *Proc. Natl. Acad. Sci. USA*, **72**, 4008-4012.
Leder,P., Battey,J., Lenoir,G., Moulding,C., Murphy,W., Potter,H., Stewart,T. and Taub,R. (1983) *Science (Wash)*, **222**, 765-770.
Miller,A.D., Curran,T. and Verma,I.M. (1984) *Cell*, **36**, 51-60.
Muller,R., Slamon,D.J., Tremblay,J.M., Cline,M.J. and Verma,I.M. (1982) *Nature*, **299**, 640-644.
Neel,B.G., Hayward,W.S., Robinson,H.L., Fang,J. and Astrin,S.M. (1981) *Cell*, **23**, 323-334.
Neil,J.C., Hughes,D., McFarlane,R., Wilkie,N.M., Onions,D.E., Lees,G. and Jarret,O. (1984) *Nature*, **308**, 814-820.
Nobis,P. and Jaenisch,R. (1980) *Proc. Natl. Acad. Sci. USA*, **77**, 3677-3681.
Nusse,R. and Varmus,H.E. (1982) *Cell*, **31**, 99-109.
Nusse,R., van Ooyen,A., Cox,D., Fung,Y.K.T. and Varmus,H. (1984) *Nature*, **307**, 131-136.
Payne,G.S., Bishop,J.M. and Varmus,H.E. (1982) *Nature*, **295**, 209-214.
Pederson,F.S., Buchhagen,D.L., Chen,C.Y., Hays,E.F. and Haseltine,W.A. (1980) *J. Virol.*, **35**, 211-218.
Peters,G., Brookes,S., Smith,R. and Dickson,C. (1983) *Cell*, **33**, 369-377.
Quint,W., Quax,W., van der Putten,H. and Berns,A. (1981) *J. Virol.*, **39**, 1-10.
Reddy,E.P., Reynolds,R.K., Santos,E. and Barbacid,M. (1982) *Nature*, **300**, 149-152.
Rowe,W.P. and Pincus,T. (1972) *J. Exp. Med.*, **135**, 429-436.
Selten,G., Cuypers,H.T., Zijlstra,M., Melief,C. and Berns,A. (1984) *EMBO J.*, **3**, 3215-3222.
Shih,C.K., Linial,M., Goodenow,M.M. and Hayward,W.S. (1984) *Proc. Natl. Acad. Sci. USA*, **81**, 4697-4701.
Steffen,D. and Weinberg,R.A. (1978) *Cell*, **15**, 1003-1010.
Tabin,C.J., Bradley,S.M., Bargmann,C.I., Weinberg,R.A., Papageorge,A.G., Scolnick,E.M., Dhar,R., Lowy,D.R. and Chang,E.H. (1982) *Nature*, **300**, 143-149.
Thomas,P.S. (1980) *Proc. Natl. Acad. Sci. USA*, **77**, 5201-5205.
van Beveren,C., Goddard,J.G., Berns,A. and Verma,I. (1980) *Proc. Natl. Acad. Sci. USA*, **77**, 3307-3311.
van Beveren,C., Rands,E.E., Chattopadhyay,S.K., Lowy,D.R. and Verma,I. (1982) *J. Virol.*, **41**, 542-556.
van der Putten,H., Terwindt,E., Berns,A. and Jaenisch,R. (1979) *Cell*, **18**, 109-116.
van der Putten,H., Quint,W., van Raay,J., Robanus Maandag,E., Verma,I. and Berns,A. (1981) *Cell*, **24**, 729-739.
Westaway,D., Payne,G. and Varmus,H.E. (1984) *Proc. Natl. Acad. Sci. USA*, **81**, 843-847.

Received on 9 April 1985